# Preprints.org

Article

# Low-Cost, Open-Source Device for Simultaneously Subjecting Rodents to Different Circadian Cycles of Light, Food, and Temperature

Ramon Farré [*] , Miguel A. Rodríguez-Lázaro , Jorge Otero , Núria Gavara , Raimon Sunyer , Nuria Farré , David Gozal , Isaac Almendros

*Article*

# Low-Cost, Open-Source Device for Simultaneously Subjecting Rodents to Different Circadian Cycles of Light, Food, and Temperature

**Ramon Farré [1,2,3,*], Miguel A. Rodríguez-Lázaro [1], Jorge Otero [1,2,4], Núria Gavara [1,4], Raimon Sunyer [1,5], Núria Farré [6,7], David Gozal [8] and Isaac Almendros [1,2,3]**

[1] Unit of Biophysics and Bioengineering, School of Medicine and Health Sciences, University of Barcelona, Barcelona, Spain;
[2] CIBER de Enfermedades Respiratorias, Barcelona (CIBERES), Barcelona, Spain;
[3] Institut Investigacions Biomèdiques August Pi Sunyer (IDIBAPS), Barcelona, Spain;
[4] The Institute for Bioengineering of Catalonia (IBEC), The Barcelona Institute of Science and Technology (BIST), Barcelona, Spain;
[5] CIBER de Bioingeniería, Biomateriales y Nanomedicina (CIBER-BBN), Barcelona, Spain;
[6] Discipline of Cardiology. Saolta University Health Care Group, Galway, Ireland;
[7] School of Medicine, University of Galway, Ireland;
[8] Office of the Dean, Joan C. Edwards School of Medicine, Marshall University, Huntington, WV 25701, USA.
[*] Correspondence: rfarre@ub.edu

**Abstract:** Exposure of experimental rodents to controlled cycles of light, food, and temperature is important when investigating alterations in circadian cycles that profoundly influence health and disease. However, applying such stimuli simultaneously is difficult in practice. Our aim was to design, build, test, and open-source describe a simple device that subjects a conventional mouse cage to independent cycles of physiologically relevant environmental variables. The device is based on a box enclosing the rodent cage to modify the light, feeding, and temperature environments. The device provides temperature-controlled air conditioning (heating or cooling) by a Peltier module and includes programmable feeding and illumination. All functions are set by a user-friendly front panel for independent cycle programming. Bench testing with a model simulating the $CO_2$ production of mice in the cage showed: a) suitable air renewal (by measuring actual ambient $CO_2$), b) controlled realistic illumination at the mouse enclosure (measured by a photometer), c) stable temperature control, and d) correct cycling of light, feeding, and temperature. The cost of all the supplies (retail purchased by e-commerce) was < 300 US$). Detailed technical information is open-source provided, allowing for any user to reliably reproduce or modify the device. This approach can considerably facilitate circadian research since using one of the described low-cost devices for any mouse group with a given light-food-temperature paradigm allows for all the experiments to be performed simultaneously, thereby requiring no changes in the light/temperature of a general-use laboratory.

**Keywords:** circadian alteration; light cycle; intermittent fasting; temperature cycle; animal research; experimental model; open-source hardware

## 1. Introduction

Like all mammals and most organisms, the human body experiences the influence of the 24-hour day/night cycle caused by Earth's rotation [1]. This circadian cycle entails periodic changes in ambient light and temperature and modulates the temporal pattern of sleep and food ingestion [2]. Homeostasis is perfectly adapted to such environmental oscillations by a system of circadian regulatory genes present not only in neurons of the suprachiasmatic nucleus but in virtually all peripheral cells [3]. Consequently, alterations in the ambient circadian cycle perturb the expression of circadian genes and thus homeostasis [4], potentially causing or aggravating a wide range of end-

organ dysfunctions, e.g., metabolic [5], insulin resistance [6], neurocognitive [7], vascular [8], cardiac [9], renal [10], fertility [11], or cancer [12].

Most research on the mechanisms determining the physiological adaptation to the circadian cycle, and the disruptions induced by circadian alterations, is carried out in animals, mainly in rodents, using relatively simple experimental settings. Indeed, modifying the timing of lab room illumination mimics alterations in the light/dark cycle, timed feeders can impose changes in food ingestion patterns, and setting the programmable thermostat in the lab room air-conditioning allows for modifying the ambient temperature cycles. However, performing experiments that better mimic real life by simultaneously combining alterations in the cycles of light, food ingestion, and ambient temperature is difficult given the common logistic and practical issues that arise from such experiments.

Specifically, studies comparing the impact of different combinations of light and temperature patterns would require changing the ambient conditions of the lab room for each group of mice being subjected to a given specific ambient paradigm. This would make it impossible to carry out the experiments in all the different groups simultaneously and would prevent using the animal facility room for other concurrent mouse experiments under conventional light and temperature conditions. Therefore, we aimed to design a device that would apply to any single rodent cage to create a specific ambient paradigm (regarding light, feed, and temperature cycling) so that different circadian conditions can be applied simultaneously to several animal groups within any single laboratory room. Notably, the solution we provide is simple, low-cost, easily scalable and, since we present it in an open-source format [13], it is freely adaptable by any interested research team.

## 2. Results

A general perspective of the specific box implemented to enclose the rodent cage and modify its environment and the control unit to set the cycling parameters are both shown in Figure 1. The material of the box walls is opaque to isolate the animals from external light and with low thermal conductivity to facilitate temperature control. Figure 2 shows the front panel of the control unit which allows the user to set and monitor the cycling variables. Figure 2 also shows the box open to present the components within the device. Illumination inside the mouse cage box is provided by intensity-controlled light-emitting diodes (LEDs), a customized on/off feeder is placed inside the mouse cage to control food availability, and a simple air-conditioning (A/C) unit allows to modulate the temperature within the box (either below or above room temperature). The air inside the box is renewed by a fan and an exhaust orifice (Figures 1 and 2).
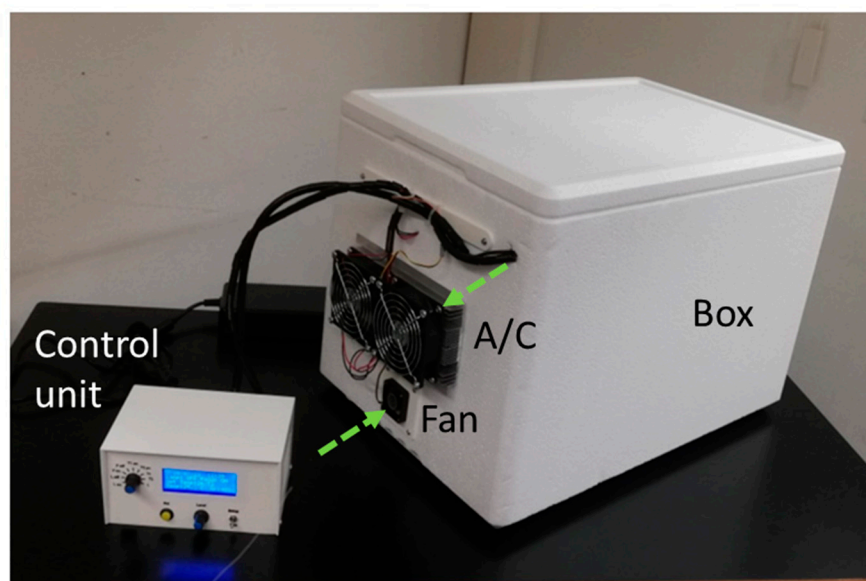
**Figure 1.** General view of the setting, showing the box to enclose the mouse cage, the control unit, the external part of the Peltier-based air conditioning (A/C) unit, the fan for introducing room air into the box, and the wall orifice used for passing the electrical lines that also serves as the outlet of the air renewal system (green arrows represent the airflow).
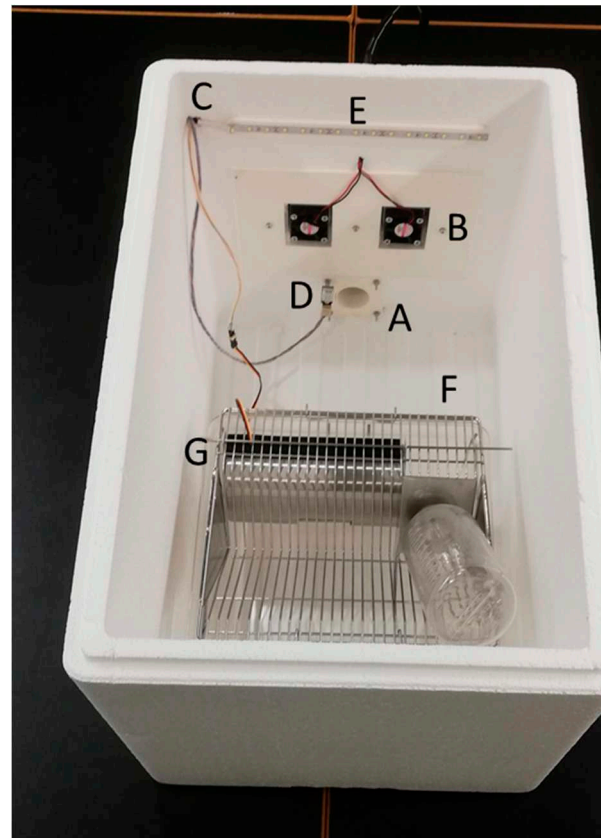


**Figure 2.** Left: Front panel of the control unit. Right: Internal top view of the box showing the conventional mouse cage incorporating the on/off feeder (G), the internal blowers of the air conditioning unit (B), the illumination LEDs (E), the temperature sensor (D), the entrance for the air renewal from the fan (placed at the external side of the wall) (A), and the orifice used for passing electrical lines and used as the air outlet (C). **.**

Photographs of the on-off feeder built to control food availability when placed inside a conventional mouse cage, and a detailed view of the feeder (from the mouse perspective), when food is available and unavailable, are shown in Figure 3. The transition time between both positions is 30 s to minimally disturb the animals.
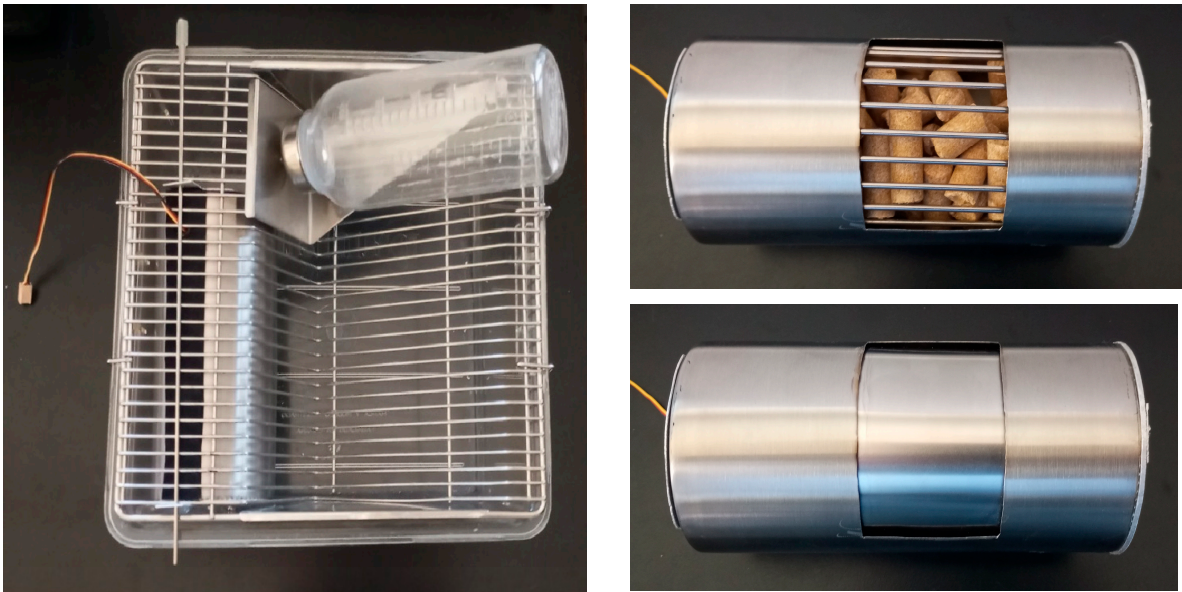
**Figure 3.** <u>Left:</u> On/off feeder inside the mouse cage placed with the window oriented to the bottom of the cage for facilitating animal access. <u>Right:</u> Feeder perspective as seen by the mice, with the window open (top) and closed (bottom) making food available and unavailable to them, respectively.

The control panel of the device allows the user to set the time-pattern type of illumination, its peak value, and the daytimes for starting and finishing the illumination period. Illuminance across different points in the bottom of the mouse cage was uniform with small variations (±30) lux depending on the exact position. Figure 4 shows examples of the on/off and progressive patterns of illumination at the bottom of the mouse cage.
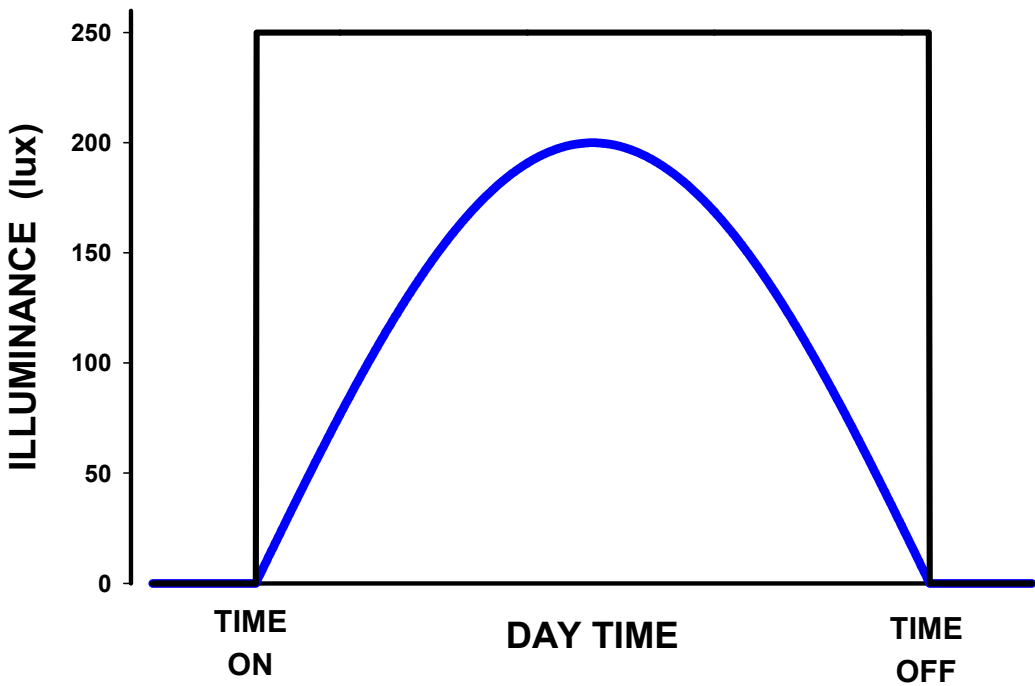


**Figure 4.** Two examples of the selectable illumination patterns applied to mice. The user can select whether the light pattern is constant (black) or progressive thus mimicking natural solar light (blue).

The daytime of light on and off, and the illuminance amplitude in lux (250 and 200 lux, respectively, in the examples) can also be set by the user.

The A/C system allowed the application of a controlled temperature cycling inside the box. The temperature could effectively be cycled within ±10 °C around the room temperature regardless of the normal oscillations of the lab room temperature, as shown in Figure 5 when the temperature was set to cycle between 18 °C and 32 °C. Of note, completely opening the box by retiring its lid for 1 min (e.g., for manipulating the mice cage) induced box temperature changes lower than 1 °C.
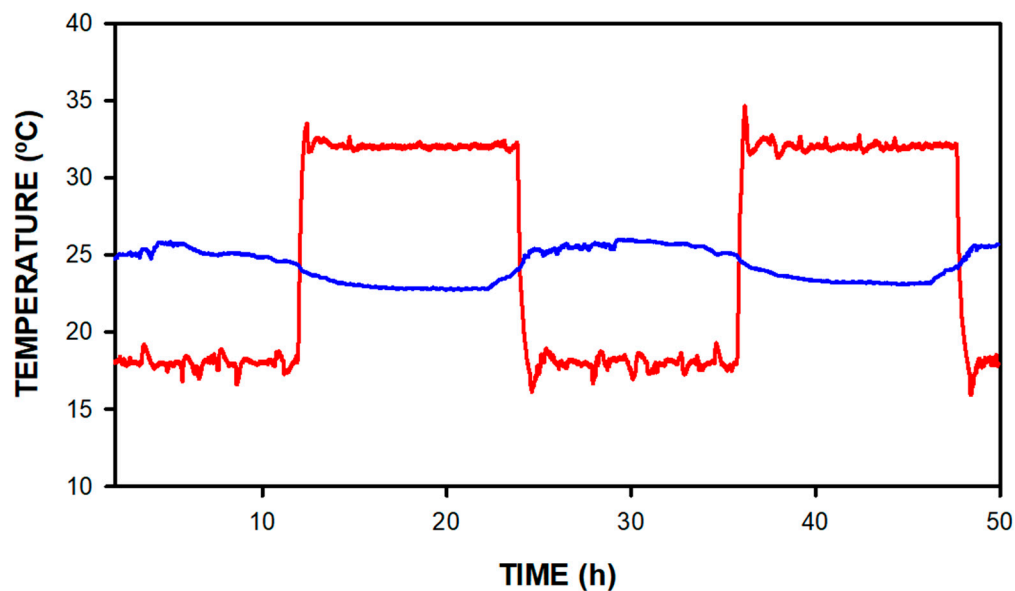


**Figure 5.** Example of raw temperatures recorded in the box (red line) and the room (blue line) when the device was normally working for 48 h for box temperature set to cycle between 18 °C and 32 °C.

Performance testing showed that under working conditions when 10 ml·min$^{-1}$ of $CO_2$ mimicking mice production was introduced into the mouse cage, the measured $CO_2$ concentration inside the box increased by only less than 500 ppm above that of the lab ambient air. Figure 6 shows that at times 0-3 min, box $CO_2$ concentration was the same as in the room air (≈510 ppm) since the fan injected room air into the box. However, at time 3 min, a continuous flow of 10 ml·min$^{-1}$ of $CO_2$ was injected into the mouse cage simulating the amount of $CO_2$ produced by 5 mice. As expected, $CO_2$ concentration started to increase until achieving a steady state of only ≈990 ppm after approximately 8 min. This recording shows that the renewal airflow through the box kept the increase in $CO_2$ concentration within a safe threshold (< 500 ppm) above the reference room air value.
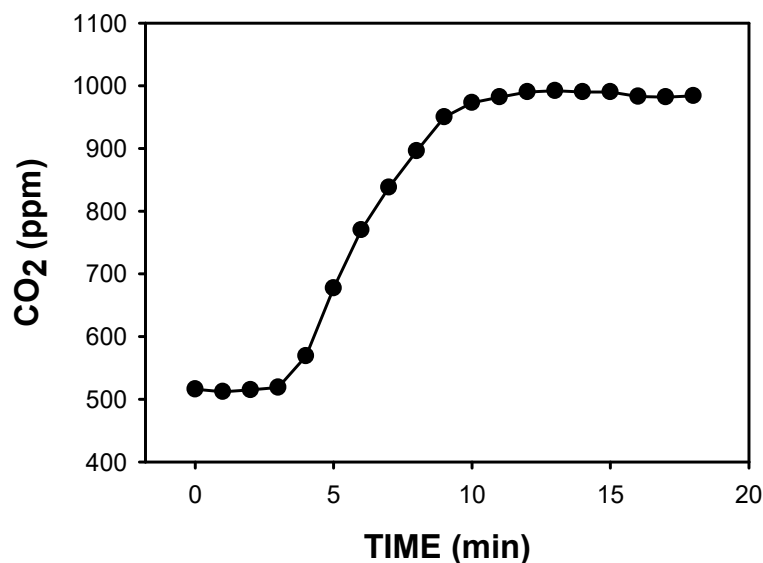
**Figure 6.** Change in $CO_2$ concentration inside the box when a continuous flow of $CO_2$ mimicking the production by 5 mice (10 ml·min$^{-1}$) was injected into the mouse cage at min 3. $CO_2$ concentration increases by less than the safe threshold of 500 ppm above the room air value.

**Discussion**

In this work, we have designed, built, bench tested, and open-source described a simple device that enables a conventional mouse cage to deliver independent cycles of physiologically relevant environmental variables. This approach can considerably facilitate integrative physiology research regarding ambient variables and the circadian cycle. Indeed, using one of the low-cost devices described here for any group of mice with a given light-food-temperature paradigm could allow performing all the experiments simultaneously with no changes required in the light/temperature of the room lab, hence allowing it to be used concurrently for mouse experiments under conventional ambient conditions. Remarkably, only general-purpose and cheap components available via e-commerce are employed, and the device construction needs only simple mechanical and electronic tools, requiring technical training not higher than the level of a bachelor in engineering.

Although we could have used any commercially available programmable feeder in our setting, we designed and built a specific one from simple materials to reduce the cost. Our solution has all parts accessible to mice made of stainless steel to prevent them from gnawing, and to allow for optimal cleaning. In addition, the feeder allows easy chow refilling and can be placed vertically or horizontally in any cage.

The illuminance at the site where mice reside is set by the conventional procedure for dimming LEDs by modifying the duty cycle of the PWM signal powering them, on the basis that pulse-width modulated (PWM) frequency (490 Hz in our case) is much higher than the visual critical flicker frequency [15]. An interesting feature of the setting described here is that in addition to the most common on/off illumination regime employed in rodent research labs, it also provides an illumination option consisting of a smooth dark-to-light transition and vice versa realistically mimicking the natural daily cycle paradigm from sunrise to sunset. This illumination option is of particular interest in investigating the specific dynamics of adaptation to the circadian light cycle [16]. Moreover, the setting can use LEDs with different types of white spectra or color light to study the potential effects of the wavelength on circadian adaptation [17,18].

To refrigerate the box, we selected an A/C unit based on an easy-to-mount, commercialized module based on the Peltier effect. Although this electrothermal procedure is energetically less efficient than conventional refrigeration by gas compression/expansion, this technology is the most suitable, simple and cheap for our specific application, which requires a relatively low refrigeration

power. Indeed, the energy rate necessary for maintaining a refrigerated box at temperature $T_{box}$ when the external temperature is $T_{ext}$ ($>T_{box}$) requires counteracting the heat transfer through the box walls ($W'_{wall}$), the heat involved in changing the temperature of external airflow V' from $T_{ext}$ to $T_{box}$ ($W'_{air}$), and the heat dissipated by mice metabolism ($W'_{met}$). According to the equation of heat transfer across a flat wall separating two compartments at different temperatures, and taking into account the total surface area and width of the box's expanded polystyrene foam walls and its thermal conductivity (35 mW·(K·m)$^{-1}$), $W'_{wall} \approx 1.7$ W per each °C in the temperature difference $T_{ext} - T_{box}$. $W'_{air}$ can be computed by considering the air density (1.2 g·l$^{-1}$) and specific heat capacity (1 J·(g·°C)$^{-1}$), resulting in $W'_{air} \approx 0.4$ W per each °C in $T_{ext} - T_{box}$. Estimation of $W'_{met}$ is not so straightforward since the dissipation of metabolic heat by mice depends on their ambient temperature ($T_{box}$) [19–21]. Whereas at 22 °C, the heat dissipation that would correspond to 5 mice is only $W'_{met} \approx 0.8$ W [21], in the case that the ambient temperature ($T_{box}$) decreases by 10 °C, $W'_{met}$ can be doubled [20]. However, even in the worst case, $W'_{met}$ would be negligible compared to $W'_{wall} + W'_{air}$, which would amount to $\approx 22$ W for a temperature difference $T_{ext} - T_{box} = 10$ °C. Hence, the Peltier module we employed (120 W) can provide the necessary refrigeration power, even when considering the relatively low efficiency of this cooling procedure. However, a Peltier module with higher power can be used if required, for instance, to target a relatively low $T_{box}$ (e.g., 5 °C) or when using an increased box size. Interestingly, reducing thermal loss can be achieved by using a box with a wider polystyrene wall or by recovering the current one with supplementary polystyrene panels. Of note, a plastic window covered by a removable polystyrene piece can be built into the box lid to periodically observe the animals while keeping the temperature unaffected. We have here focused on the cooling function of the A/C setting since operating the Peltier effect as a heater is much more efficient and poses no potential problems.

We chose a very conservative and safe limit (a maximum of 500 ppm above the lab air level) for the accepted increase in $CO_2$ levels within the box. As the metabolic $CO_2$ production by five mice (10 ml$_{CO_2}$·min$^{-1}$) should equal the difference in $CO_2$ content in the air renewal flow V' at the entrance and outlet of the box (i.e., V' × 5 × 10$^{-4}$ ml$_{CO_2}$·ml$_{air}$$^{-1}$), it follows that to keep the 500 ppm maximum increase, the renewal airflow circulated should be V' $\approx 20$ l$_{air}$·min$^{-1}$. This flow is 2,000 fold the 5-mice $CO_2$ production flow, a figure that would correspond to V' = 500 l·min$^{-1}$ for a typical human (250 ml$_{CO_2}$·min$^{-1}$ of $CO_2$ production), which almost doubles the 5 l·s$^{-1}$ (300 l·min$^{-1}$) per person recommended for ventilation in buildings [22]. In practical terms, it was not necessary to measure V' because we verified its effectiveness for air renewal by simply measuring the $CO_2$ concentration inside the cage with a conventional sensor. The small fan employed had a nominal flow of $\approx 140$ l·min$^{-1}$ in open air, which is much higher than required (20 l$_{air}$·min$^{-1}$). However, when subjected to the impedance of the entrance and outlet orifices for air renewal the flow generated by this type of fan (which is not a pressure generator blower) is strongly dampened. As a result, the orifices we set for the air renewal pathway proved to satisfactorily keep safe $CO_2$ levels inside the box. Of note, in addition to maintaining an adequate $CO_2$ level within the box, the renewal airflow V' also compensates for the $O_2$ consumption by mice metabolism. Given that the flow rate of $O_2$ consumption is similar to that of $CO_2$ production (respiratory exchange ratio $\approx 1$) [21], a given V' would entail a decrease in the $O_2$ fraction within the box similar to the corresponding increase in $CO_2$ fraction. Hence, assuming a 500 ppm change relative to room air would negligibly reduce the $O_2$ concentration in the box from $\approx 21\%$ to $\approx 20.95\%$.

**4. Materials and Methods**

*4.1. Device description.*

Figure 7A shows a general schematic of the box. The specific implementation we present herein (Figure 1) can accommodate either a conventional mouse cage (28 x 28 x 16 cm) or a cage (40.6 x 26.7 x 36.8 cm) for subjecting mice to sleep fragmentation/deprivation (model 80391, Lafayette Instruments, Lafayette, IN) [23,24]. To this end, we used an expanded polystyrene foam box (external 59.5 x 39.5 x 40 cm, 3 cm wall width; Broxon GmbH via Amazon) commercialized for food

temperature maintenance. A 4-cm diameter personal computer fan (FAN4, AABCOOLING, via Amazon) continuously circulates room air through the box for air renewal.
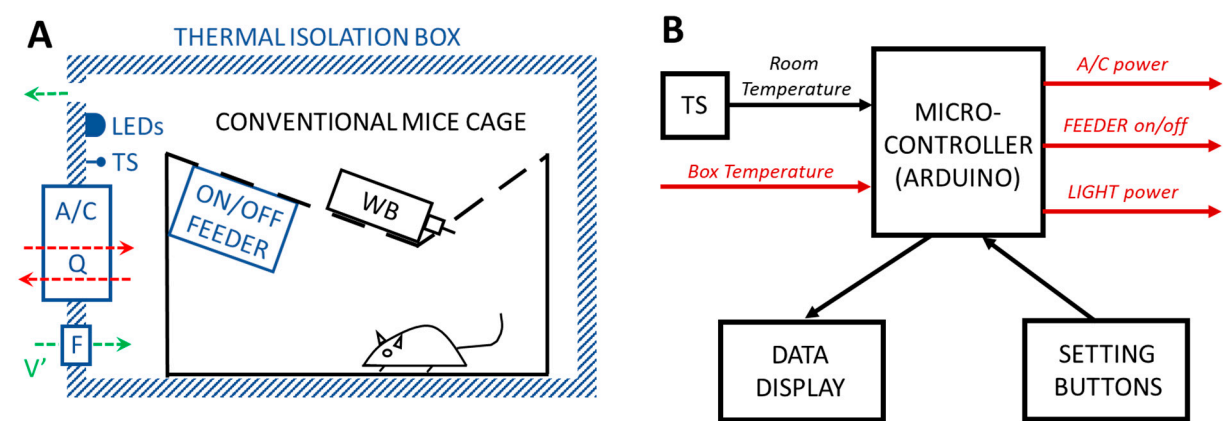


**Figure 7.** Diagram of the device. (A) A conventional mouse cage with a water bottle (WB) is enclosed inside an opaque and thermal isolation box. Warm-white LEDs and a temperature sensor (TS) are placed inside the box. An air-conditioning (A/C) Peltier-based module is placed through the box wall, allowing heat (Q) to flow (red arrows) from the box to the room and vice versa when acting as a cooler or heater, respectively. An on/off feeder allows for controlling food availability. A fan and an orifice in the box walls allow continuous airflow (V') for air renewal (green arrows). (B) A microcontroller drives the cycling of A/C, feeder, and light based on the box and the room temperature (measured by a temperature sensor (TS)) and according to the settings established by the user. Signals from/to the box in red color. See the text for a detailed explanation.

A circuit (Figure 7B), based on an Arduino Nano microcontroller (Arduino, via Amazon) and a real-time clock unit (DS1307 RTC I2C, Fasici, via Amazon), is placed into a 3D-printed PLA enclosure box to control the device. The box's front panel has displays and buttons allowing the user to independently set the cycling times for light and feeding and the temperatures and times for the thermal cycles (see details in Supplementary Materials).

A customized feeder to control food availability for mice was built using cheap, commonly available, easy-to-mechanize materials (Figure 8). All the surfaces potentially in contact with mice are made from stainless steel. We cut the external cylinder (81-mm diameter, 170-mm height) from a stainless-steel beverage bottle (1-liter, Tripple Tree via Amazon), and we made the internal cage for containing conventional mice chow by using 3D-printed polylactic acid (PLA) pieces (covered with 0.1-mm width stainless steel foil where required) and stainless-steel bars (2.5-mm diameter). Mice have access to food depending on the relative position of the internal cage vs. the external windowed cylinder. Rotating the internal cage with a servomotor (commercialized for aeromodelling) (HS-325HB, HITEC, via Amazon) changes the on/off feeding state.
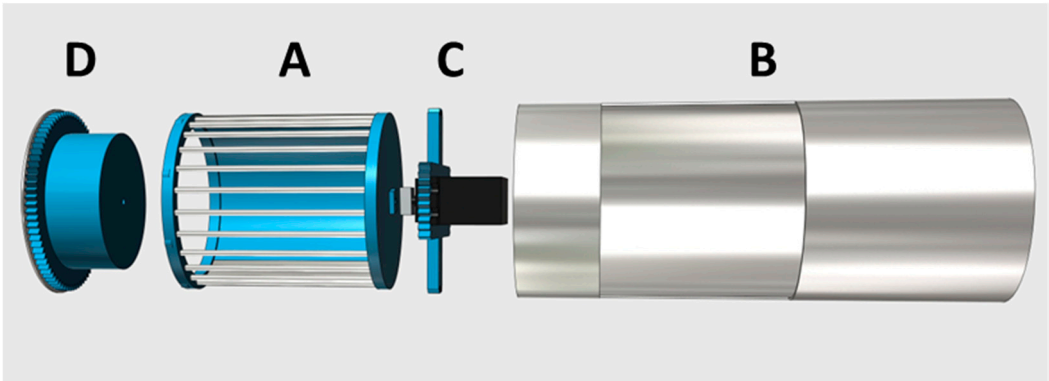
**Figure 8.** Diagram of unmounted pieces of the on/off feeder. A: internal cylinder to contain the conventional mice chop. One lateral part is made with stainless steel bars and the other lateral part is 3D-printed PLA (internal) and stainless steel (external, not seen in the figure). B: External cylinder with a window. C: Piece to be connected to the internal cylinder. D: 3D-printed cap. E: the place for a rotating motor. When the pieces are mounted (by displacing them from left to right), the internal cylinder can rotate inside the external one, allowing the mice (in front of the window of the external cylinder) to access the chop when the internal cylinder presents its lateral side with bars or preventing chop access when presenting the stainless-steel wall.

Fifteen LED units (12 V, warm-white 3000 K; Lighting EVER via Amazon) allow illumination into the mouse cage. To set an adequate illuminance level at the mouse location, we placed the sensing element of a photometer (DM-lx1010bsxxx, Dr. Meter via Amazon) at the bottom of the mouse cage when the box was closed in working conditions. When the LEDs were continuously powered with the 12 V tension, the local illuminance was 370 lux at the center of the mice box bottom, which is in keeping with a well-illuminated animal research lab [25]. However, any illuminance value below this figure can be achieved by further reducing the duty cycle of the 12-V pulse-width modulated (PWM) powering the LEDs as set in the front panel of the device (see Supplementary Material for user manual). The device allows selecting one of two different time patterns of illumination: a simple on/off or a half-wave rectified sine simulating the progressive increase/decrease of intensity along the day [26] (Figure 4). It should be mentioned that the 3-cm polystyrene foam wall of the box is not completely opaque. For instance, when the closed box was placed in a well-illuminated room (≈ 600 lux) and the LEDs switched off), the illuminance at the mice site was ≈ 15 lux. In the case of aiming for a completely darker nocturnal period, the box walls can simply be painted black or lined with an opaque plastic/cardboard sheet.

A Peltier cooling module, typically commercialized for cooling microprocessors inside computers (120 W, 12 V, TEC1-12706, YWBL-WH, via Amazon), is placed through the box wall, with the cooling and heating sides (both including fans continuously working regardless of heating/cooling) inside and outside the box, respectively. The A/C fans in the internal side of the box contribute to homogenizing the gas composition by mixing air renewal flow and mice breathing gases). When a nominal positive voltage of 12 V powers the Peltier module, it reduces the temperature inside the box. However, when this A/C unit is powered with a negative voltage, the heat flow is inverted, and the box is heated. The polarity of the power applied to the Peltier module, and thus whether it works to cool or heat the box, is determined by the microcontroller depending on whether the room temperature sensed by a thermometer (SHT21 HTU21, HiLetgo, via Amazon) is higher or lower than the setting for box temperature, respectively. The microprocessor uses another thermometer (SHTC3, Youmile, via Amazon) inside the box to control the on/off operation of the A/C unit.

*4.2. Performance test.*

We assessed the device's performance under real-life conditions in well-controlled bench conditions freed from biological variability. The most relevant issue to test was the interaction between box temperature and air renewal flow (V'). Indeed, each of these variables conflicts with the other since excessively increasing V' may compromise the capacity of the A/C system to control temperature. On the contrary, a too-poor air renewal may excessively increase $CO_2$ inside the mouse cage. Therefore, we realistically mimicked the $CO_2$ produced by five mice (a typical number for the cage employed) by introducing a $CO_2$ flow of 10 ml·min$^{-1}$ at the mouse cage bottom using narrow tubing and a servo-controlled gas blender (McQ, Virginia, USA). We established this value by assuming 30-g mice and that $CO_2$ production by mouse metabolism is 4 $l_{CO_2}$·(h·g)$^{-1}$ [21]. According to conventional regulations [27], we aimed to limit any increase in the box $CO_2$ concentration to 500 ppm (i.e., $5 \times 10^{-4}$ $ml_{CO_2}$·$ml_{air}^{-1}$) above the room $CO_2$ level (which means increasing the $CO_2$ fraction in the air by 0.05%). To test the device performance under such realistic conditions, we measured the actual $CO_2$ concentrations both in the room air and inside the cage using a commercially available $CO_2$ sensor (Dioxcare DX700 PDF, Girona, Spain).

*4.3. Construction details.*

All the components used to build the device were retail purchased via e-commerce (Amazon or Alibaba). The total cost of the device components, including the microprocessor, electrical and electronic components, power source, box, and mechanical parts, was < 300 € (i.e., < 300 US$) As the design is modular and all components are commercialized for general purpose use, they are easy to find and to be replaced by others with similar features if required. The construction is robust and its routine operation does not require the use of consumables. The energy consumption is low on a daily average (mainly depending on the lowest temperature set), with a peak of just 150 W during the phases of maximum cooling.

Full details of the electronic components, circuits and connections, mechanical pieces and their assembly, 3D-printer codes for parts and for the enclosure box, the Arduino control code, and a user manual, are freely undisclosed and available in the Supplementary Materials so that any interested user can replicate the device or adapt it to specific needs.

## 5. Conclusions

In conclusion, we provide a detailed and free technical description of an easy-to-reproduce device for simultaneously subjecting rodents to different circadian cycles of light, food, and temperature. Among the possible simple changes required to further enlarge the applicability of the device is the use of a larger box to allow a variety of experimental settings. For instance, to host rats or more mice, to provide them with enhanced hosting [22,29], or to include devices for precisely dosing/weighing food intake [30], monitoring animal movements [31,32], or to allow animals to exercise [33,34].

## References

1. Stanton D, Justin HS, Reitzel AM. Step in Time: Conservation of Circadian Clock Genes in Animal Evolution. Integr Comp Biol. 2022 Dec 30;62(6):1503-1518. https://doi.org/10.1093/icb/icac140.
2. Fishbein AB, Knutson KL, Zee PC. Circadian disruption and human health. J Clin Invest. 2021 Oct 1;131(19):e148286. https://doi.org/10.1172/JCI148286.
3. Fagiani F, Di Marino D, Romagnoli A, Travelli C, Voltan D, Di Cesare Mannelli L, Racchi M, Govoni S, Lanni C. Molecular regulations of circadian rhythm and implications for physiology and diseases. Signal Transduct Target Ther. 2022 Feb 8;7(1):41. https://doi.org/10.1038/s41392-022-00899-y.
4. Xie Y, Tang Q, Chen G, Xie M, Yu S, Zhao J, Chen L. New Insights Into the Circadian Rhythm and Its Related Diseases. Front Physiol. 2019 Jun 25;10:682. https://doi.org/10.3389/fphys.2019.00682.
5. Gutierrez Lopez DE, Lashinger LM, Weinstock GM, Bray MS. Circadian rhythms and the gut microbiome synchronize the host's metabolic response to diet. Cell Metab. 2021 May 4;33(5):873-887. https://doi.org/10.1016/j.cmet.2021.03.015.
6. Stenvers DJ, Scheer FAJL, Schrauwen P, la Fleur SE, Kalsbeek A. Circadian clocks and insulin resistance. Nat Rev Endocrinol. 2019 Feb;15(2):75-89. https://doi.org/10.1038/s41574-018-0122-1.
7. Yalçin M, Mundorf A, Thiel F, Amatriain-Fernández S, Kalthoff IS, Beucke JC, Budde H, Garthus-Niegel S, Peterburs J, Relógio A. It's About Time: The Circadian Network as Time-Keeper for Cognitive Functioning,

Locomotor Activity and Mental Health. Front Physiol. 2022 Apr 25;13:873237. https://doi.org/10.3389/fphys.2022.873237.

8. Han Q, Bagi Z, Rudic RD. Review: Circadian clocks and rhythms in the vascular tree. Curr Opin Pharmacol. 2021 Aug;59:52-60. https://doi.org/10.1016/j.coph.2021.04.010.

9. Delisle BP, George AL Jr, Nerbonne JM, Bass JT, Ripplinger CM, Jain MK, Hermanstyne TO, Young ME, Kannankeril PJ, Duffy JF, Goldhaber JI, Hall MH, Somers VK, Smolensky MH, Garnett CE, Anafi RC, Scheer FAJL, Shivkumar K, Shea SA, Balijepalli RC. Understanding Circadian Mechanisms of Sudden Cardiac Death: A Report From the National Heart, Lung, and Blood Institute Workshop, Part 1: Basic and Translational Aspects. Circ Arrhythm Electrophysiol. 2021 Nov;14(11):e010181. https://doi.org/10.1161/CIRCEP.121.010181.

10. Mohandas R, Douma LG, Scindia Y, Gumz ML. Circadian rhythms and renal pathophysiology. J Clin Invest. 2022 Feb 1;132(3):e148277. https://doi.org/10.1172/JCI148277.

11. Sciarra F, Franceschini E, Campolo F, Gianfrilli D, Pallotti F, Paoli D, Isidori AM, Venneri MA. Disruption of Circadian Rhythms: A Crucial Factor in the Etiology of Infertility. Int J Mol Sci. 2020 May 30;21(11):3943. https://doi.org/10.3390/ijms21113943.

12. Qu M, Zhang G, Qu H, Vu A, Wu R, Tsukamoto H, Jia Z, Huang W, Lenz HJ, Rich JN, Kay SA. Circadian regulator BMAL1::CLOCK promotes cell proliferation in hepatocellular carcinoma by controlling apoptosis and cell cycle. Proc Natl Acad Sci U S A. 2023; 120(2):e2214829120. https://doi.org/10.1073/pnas.2214829120.

13. Farré R, Gozal D, Nguyen VN, Pearce JM, Dinh-Xuan AT. Open-Source Hardware May Address the Shortage in Medical Devices for Patients with Low-Income and Chronic Respiratory Diseases in Low-Resource Countries. J Pers Med. 2022 Sep 13;12(9):1498. https://doi.org/10.3390/jpm12091498.

14. National Research Council (US) Committee for the Update of the Guide for the Care and Use of Laboratory Animals. Guide for the Care and Use of Laboratory Animals, 8th edition. Washington (DC): National Academies Press (US); 2011. ISBN-13: 978-0-309-15400-0ISBN-10: 0-309-15400-6.

15. DeRamus ML, Kraft TW. Optimizing ERG Measures of Scotopic and Photopic Critical Flicker Frequency. Adv Exp Med Biol. 2018;1074:145-150. https://doi.org/10.1007/978-3-319-75402-4_18.

16. Crowley SJ, Eastman CI. Phase advancing human circadian rhythms with morning bright light, afternoon melatonin, and gradually shifted sleep: can we reduce morning bright-light duration? Sleep Med. 2015 Feb;16(2):288-97. https://doi.org/10.1016/j.sleep.2014.12.004.

17. Dauchy RT, Blask DE, Hoffman AE, Xiang S, Hanifin JP, Warfield B, Brainard GC, Anbalagan M, Dupepe LM, Dobek GL, Belancio VP, Dauchy EM, Hill SM. Influence of Daytime LED Light Exposure on Circadian Regulatory Dynamics of Metabolism and Physiology in Mice. Comp Med. 2019 Oct 1;69(5):350-373. https://doi.org/10.30802/AALAS-CM-19-000001.

18. Kapogiannatou A, Paronis E, Paschidis K, Polissidis A, Kostomitsopoulos NG. Effect of light colour temperature and intensity on the behaviour of male C57CL/6J mice. Applied Animal Behaviour Science, Volume 184, 2016, Pages 135-140. https://doi.org/10.1016/j.applanim.2016.08.005.

19. Gordon CJ. The mouse thermoregulatory system: Its impact on translating biomedical data to humans. Physiol Behav. 2017 Oct 1;179:55-66. https://doi.org/10.1016/j.physbeh.2017.05.026.

20. Abreu-Vieira G, Xiao C, Gavrilova O, Reitman ML. Integration of body temperature into the analysis of energy expenditure in the mouse. Mol Metab. 2015 Mar 10;4(6):461-70. https://doi.org/10.1016/j.molmet.2015.03.001.

21. Kim ER, Tong Q. Oxygen Consumption Rate and Energy Expenditure in Mice: Indirect Calorimetry. Methods Mol Biol. 2017;1566:135-143. https://doi.org/10.1007/978-1-4939-6820-6_13.

22. Olesen, B.W. & Bogatu, Dragos-Ioan & Kazanci, Ongun & Coakley, Daniel. (2021). The use of CO2 as an indicator for indoor air quality and control of ventilation according to EN16798-1 and TR16798-2. Paper presented at 15th ROOMVENT Conference. https://orbit.dtu.dk/en/publications/the-use-of-cosub2sub-as-an-indicator-for-indoor-air-quality-and-c

23. Cabrera-Aguilera I, Benito B, Tajes M, Farré R, Gozal D, Almendros I, Farré N. Chronic Sleep Fragmentation Mimicking Sleep Apnea Does Not Worsen Left-Ventricular Function in Healthy and Heart Failure Mice. Front Neurol. 2020 Jan 9;10:1364. https://doi.org/10.3389/fneur.2019.01364.

24. Farré R, Almendros I, Martínez-García MÁ, Gozal D. Experimental Models to Study End-Organ Morbidity in Sleep Apnea: Lessons Learned and Future Directions. Int J Mol Sci. 2022 Nov 20;23(22):14430. https://doi.org/10.3390/ijms232214430.

25. Dauchy RT, Blask DE. Vivarium Lighting as an Important Extrinsic Factor Influencing Animal-based Research. J Am Assoc Lab Anim Sci. 2023 Jan 1;62(1):3-25. https://doi.org/10.30802/AALAS-JAALAS-23-000003.

26. Oteiza P, Pérez-Burgos A. Diffuse illuminance availability on horizontal and vertical surfaces at Madrid, Spain. Energy Conversion and Management, 64: 313-319, 2012. https://doi.org/10.1016/j.enconman.2012.05.022.

27. American Society of Heating, Refrigerating and Air-Conditioning Engineers (ASHRAE). ASHRAE Position Document on Indoor Carbon Dioxide. Approved by ASHRAE Board of Directors, February 2, 2022.

https://www.ashrae.org/file%20library/about/position%20documents/pd_indoorcarbondioxide_2022.pdf. Last download on July 2, 2023.

28. Makowska IJ, Weary DM. A Good Life for Laboratory Rodents? ILAR J. 2021 Sep 24;60(3):373-388. https://doi.org/10.1093/ilar/ilaa001. PMID: 32311030.

29. Cait, J., Cait, A., Scott, R.W. et al. Conventional laboratory housing increases morbidity and mortality in research rodents: results of a meta-analysis. BMC Biol 20, 15 (2022). https://doi.org/10.1186/s12915-021-01184-0.

30. Ali MA, Kravitz AV. Challenges in quantifying food intake in rodents. Brain Res. 2018 Aug 15;1693(Pt B):188-191. https://doi.org/10.1016/j.brainres.2018.02.040.

31. Genewsky A, Heinz DE, Kaplick PM, Kilonzo K, Wotjak CT. A simplified microwave-based motion detector for home cage activity monitoring in mice. J Biol Eng. 2017 Nov 16;11:36. https://doi.org/10.1186/s13036-017-0079-y.

32. Matikainen-Ankney BA, Garmendia-Cedillos M, Ali M, Krynitsky J, Salem G, Miyazaki NL, Pohida T, Kravitz AV. Rodent Activity Detector (RAD), an Open Source Device for Measuring Activity in Rodent Home Cages. eNeuro. 2019 Jul 10;6(4):ENEURO.0160-19.2019. https://doi.org/10.1523/ENEURO.0160-19.2019.

33. Goh J, Ladiges W. Voluntary Wheel Running in Mice. Curr Protoc Mouse Biol. 2015 Dec 2;5(4):283-290. https://doi.org/10.1002/9780470942390.mo140295.

34. Kim YJ, Kim HJ, Lee WJ, Seong JK. A comparison of the metabolic effects of treadmill and wheel running exercise in mouse model. Lab Anim Res. 2020 Feb 7;36:3. https://doi.org/10.1186/s42826-019-0035-8.